Impact of the Interfacial Molecular Structure Organization on the Charge Transfer State Formation and Exciton Delocalization in Merocyanine:PC61BM Blends

Impact of the interfacial molecular structure organization on the charge transfer state formation and exciton delocalization in merocyanine:$PC_{61}BM$ blends

K. Budzinauskas[1*], D. Fazzi[2], D. Hertel[2], S. Rüth[2], J. Schelter[2], P. Weitkamp[2], K. Meerholz*[2], P. H. M. van Loosdrecht*[1]

[1]Institute of Physics 2, University of Cologne, Zülpicher Str.77, Cologne, Germany

[2]Department Chemistry, Institute of Physical Chemistry, University of Cologne, Greinstrasse 4-6, Cologne, Germany

Keywords: Aggregation, Merocyanines, Charge transfer state, Bulk heterojunction, Morphology

ABSTRACT: The intermolecular charge transfer (CT) exciton in merocyanine: [6,6]-phenyl-C_{61}-butyric acid methyl ester ($PC_{61}BM$) system, induced by the molecular geometry is investigated. The CT state, localized on the merocyanine domain, was experimentally observed in the transient spectra as well as modeled via DFT/TDDFT calculations. A relationship between molecular geometry at the Donor:Acceptor interface and the delocalization of the CT exciton was identified. It was found that different alkyl side chains of merocyanine can be used to tune the formation of H-aggregates by means of better intermixing with $PC_{61}BM$. Moreover, we observed that high H-aggregation increases the charge delocalization and improves the efficiency and carrier transport properties of the merocyanine-based bulk heterojunction solar cell.

Introduction The intermolecular interaction and packing behaviour plays a major role in organic electronics, influencing the photophysical properties of molecular materials[1–3]. Molecular packing and relative orientations can alter the exciton splitting, charge and energy transport[4,5] as well as optical[6,7] and non-linear[8–11] optical properties of organic systems as those used in organic photovoltaics (OPV). In OPV devices, photogenerated excitons dissociate across the donor/acceptor interface and form an interfacial charge transfer (CT) exciton or free charge carriers[12]. The molecular arrangement at the donor (D) / acceptor (A) interface plays a crucial role in exciton formation and dissociation dynamics. One of the most fundamentally important questions concerning self-organized molecules in OPVs is the relation between the molecular geometry and packing of donor and acceptor molecules, and their impact on the overall device performance. It is still an ongoing debate whether, for instance, face-on configuration between D and A molecules is favourable compared to edge–on configuration.[13,14] In general, it is perceived that OPV devices with face-on orientation at D:A interfaces have better performance compared with edge–on, mainly because of different ionization potentials leading to higher V_{oc}.[15–17] A number of researchers have tried to resolve this question by changing the relative orientation of molecules at D:A interfaces in solar cells.[18] Despite significant progress it remained experimentally challenging to address the local molecular packing at D:A interfaces. One way to change the packing is for instance by tuning the molecular structure through chemical engineering. One class of donor molecules, which is widely used in the field of OPV, are merocyanines which can be easily tuned chemically.[19–22] These dipolar dyes are of interest in the field of OPV because it was shown that they could increase both, the efficiency of electron-hole pair splitting and charge mobility in organic solar cells.[20,23]

The molecular packing and exciton delocalization properties are strongly interconnected: a tightly packed molecular structure can enhance the exciton delocalization. The exciton delocalization and charge transfer state formation at the donor/acceptor interface is the crucial ingredient for efficient exciton splitting at the D/A molecular interface. The optical probing of highly delocalized excitonic states is problematic because strong wavefunction delocalization leads to a weak transition dipole moment. It is possible to detect this kind of delocalized excitons via stimulated emission which is proportional to the population of the charge transfer excitons.

In this work we investigated molecular order dependent photophysical properties of merocyanine:$PC_{61}BM$ blends. Depending on the shape of alkyl chain (linear or branched) of merocyanine molecules, different molecular packing was observed. More specifically, we investigate properties of the intermolecular charge transfer exciton on merocyanine dimer and how it depends on the relative orientation between donor and acceptor molecules. In this work, both experimental and quantum-chemical computational methods show that two distinct packing motifs, namely face-on or edge-on, can be accessed using merocyanine molecules with different alkyl sidechains ultimately affecting the formation of the charge transfer state and electron-hole pair delocalisation.

Experimental details. In this study, the merocyanines 2-((Z)-4-tert-butyl-5-((E)-2-(3,3-dimethyl-1-(2-ethylhexyl)indolin-2-ylidene)ethylidene)thiazol-2(5H)-ylidene)malononitrile (**MB**, branched alkyl) and 2-((Z)-4-tert-butyl-5-((E)-2-(3,3-dimethyl-1-nonylindolin-2-ylidene)ethylidene)thiazol-2(5H)-ylidene)malononitrile (**ML**, linear alkyl), having branched and linear alkyl sidechains, respectively (see inset Fig. 1) were used. The different alkyl chains result in different molecular packing properties of the investigated dyes.

Both compounds were synthesised via established literature procedures, see supporting information (SI) for details. Thin films and devices were prepared by spin coating from chloroform solutions of 15 mg/ml in inert atmosphere on quartz. Mixed films with $PC_{61}BM$ (Solenne) had a composition of 2:3 (merocyanine:fullerene) by volume. Details of the device fabrication are given in the SI.

Absorption measurements were performed using a Lambda 1050 (Perkin Elmer) UV/vis spectrometer. A molar concentration of 10^{-4}-10^{-6} mol/l was used for performing optical absorption measurements in a solution.

Transient absorption (TA) experiments were performed using Yb:KGW based laser system Pharos (Light Conversion) with 150 kHz repetition rate and 40 fs pulse duration and internal NOPA with 800 nm and 1450 nm outputs. The 3 eV excitation pulse was generated via second harmonic generation by focusing 800 nm beam to the Beta barium borate (BBO) crystal. White light super continuum probe, was generated by focusing 1450 nm beam in to the 4mm thick Sapphire crystal.

The structural and electronic properties of **MB** and, and their molecular interfacing with $PC_{61}BM$ were computed *via* first-principles calculations at the Density Functional Theory (DFT) and time-dependent DFT (TDDFT) levels. A range-separated functional, namely ωB97X-D3, with Grimme's dispersion corrections, and a split-valence double-zeta Pope's basis set 6-31G* were adopted for each calculation. Geometry optimizations were validated by Hessian calculations, showing no imaginary frequencies for each ground state structure. A variety of structural models (e.g. from single molecules to clusters) were investigated in order to describe the excited state properties of merocyanines and their interfaces with $PC_{61}BM$. Details about all structures are reported in Supporting Information. The structural models considered (for both **MB** and **ML**) were: *i*) isolated molecules, *ii*) two interacting merocyanines (i.e., dimers, named 2x**MB** and 2x**ML**, both in parallel and antiparallel dipole configurations), *iii*) one merocyanine interfaced with one $PC_{61}BM$ (e.g. **MB**:$PC_{61}BM$), and finally *iv*) two merocyanines interfaced with one $PC_{61}BM$ (e.g. 2x**MB**:$PC_{61}BM$). For the latter, both, the *on-top* and the *on-side* positions of the $PC_{61}BM$ with respect to the merocyanine dimer were considered. The electronic structure of cyanine-based molecules is particularly challenging to model[24], involving the description of strong electron correlation effects in the excited states, usually not properly capture by TDDFT.[25] Configuration interaction approaches or DFT/GW calculations were successfully considered for describing the ground and excited states of merocyanines[24]. Hybrid range-separated DFT functionals were also applied to merocyanines and similar "zwitterionic"-like organic systems[26]. They alleviate the deficiencies of pure or hybrid DFT functionals in describing correlated systems and CT states, however they tend to overestimate the energy of the excited states (in some cases more than 1 eV). Hybrid range-separated DFT functionals were also recently applied to model the electronic structure of dimers, clusters and crystals of merocyanines similar to those investigated here[27]. Similarly to what reported in literature, for comparing the TDDFT energies with experimental values, we shifted the computed vertical transition energies by 0.8 eV[8]. All calculations on single molecules, dimers and clusters were performed with Gaussian16 (B.01 version)[28]. The absorption spectrum of **ML** crystal (Fig. 1a) was computed *via* pseudopotential plane-wave DFT calculations, using the code QuantumESPRESSO[29] coupled with the turboTDDFPT code[30]. For such a calculation, the PBE generalized gradient exchange–correlation functional and ultrasoft pseudo-potentials from the PS library were used. Single-particle wavefunctions (charge density) are expanded in planewaves up to an energy cutoff of 70 Ry (700 Ry). Only Γ point has been considered for Brillouin zone sampling in the reciprocal space[31]. The calculated spectrum is reported in Fig. 1a.

Results and discussions. The ground state dipole moment of **MB** and **ML** is 15.8 and 15.5 Debye, respectively, as derived from DFT, which compares well with experimental values of similar merocyanines.[32] Such a large dipole moment enables strong dipole-dipole interactions driving aggregate formation.

To shed light on the optical properties of **MB** and, absorption spectra in acetone were measured (Fig. 1a,b). We postulate that these correspond to monomeric molecular absorption spectra since there is no evidence of molecular aggregation. These spectra have similar spectral shape for both molecules, thus showing that different alkyl chains do not perturb the electronic structure of the molecular core unit. Both spectra show the 0-0 vibronic transition at 2.0 eV, and the 0-1 at 2.15 eV (Fig. 1a,b), i.e., the energy-spacing of these vibronic transitions is 1290 cm^{-1} (150 meV). This vibrational energy can be assigned to the C-C/C=C stretching/shrinking mode of the carbon backbone in the excited state[33].

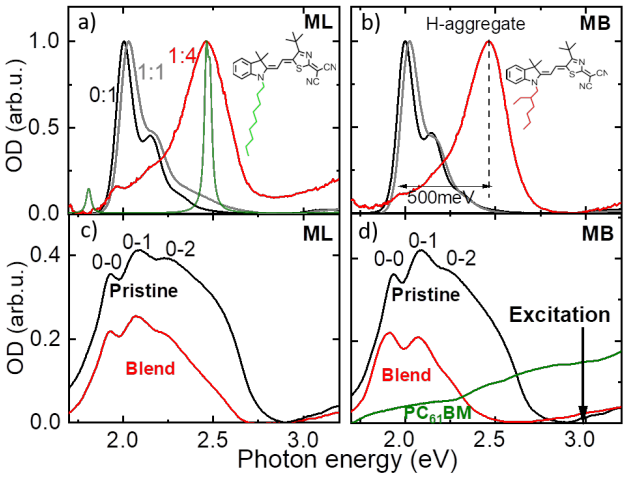

Figure 1: Absorption spectra of **ML** (a) and **MB** (b) dissolved in solvents with a 0:1(black), 1:1(grey), 1:4(red) acetone:water ratios. The gradual increase in water content leads to
H-aggregate formation (red). The green spectrum in (a) represents the computed spectrum for **ML** single crystal. Absorption spectra of thin films of **ML** (c) and **MB** (d) in pristine state (black line) and in mixture with $PC_{61}BM$ (red line), respectively. The green spectrum in (d) represents the absorption spectrum of a pure $PC_{61}BM$ film.

The intermolecular interaction between dipolar molecules can be explained by the angle-averaged Keesom force between two permanent dipoles. By changing the dielectric properties of the environment, the intermolecular interaction can be controlled. Here, we have used a mixture of solvents with different dielectric constants for achieving this control, namely water ($\epsilon_r = 80$) and acetone ($\epsilon_r = 20.7$).[34] The optical spectra of **ML** and **MB** as dissolved in solvents are shown in Fig. 1a,b. A dramatic change in the absorption spectrum occurs at 1:4 acetone:water ratio, where a strong peak at 2.5 eV appears. This hypsochromically shifted band is caused by H-type aggregate formation, due to the excitonic coupling between molecules [35,36].

The exciton coupling can be experimentally estimated from the energy difference between monomer and aggregate absorption bands. In the spectrum, the monomer absorption is at 1.85 eV whereas the aggregates absorb at around 2.4 eV. The band splitting, from which the coupling can be estimated, is shown in Fig. 1b. The deduced coupling energy J_c is 250 meV. This coupling falls in the typical energy range for (mero-)cyanine-based H-aggregates, i.e., 200 to 500 meV depending on the molecular packing and value of the transition dipole moment.[21,37,38] In Fig. 1a the computed electronic absorption spectrum of **ML** single crystal is also reported. It shows two main absorption bands, at 1.80 eV and 2.45 eV, featuring an energy splitting of 0.65 eV. The two bands are polarized along the *b*- and *c*-axis of the molecular crystal. The computed single-crystal spectrum well match the experimental spectrum of aggregated **ML** in acetone:water with a ratio of 1:4, suggesting the formation of H-aggregated particles after the solution crashes out when adding anti-solvent. In particular, the presence of a low energy (~1.8 eV) and a high energy (~2.5 eV) band in the UV-Vis spectra of films and blends (see next sections) will suggest the presence of merocyanine aggregates.

The absorption spectra of merocyanine films are shown in Fig. 1c, d. By comparing these absorption spectra with those obtained in solution (Fig. 1a, b), a strong spectral broadening in the film spectra can be observed, caused by the inhomogeneous broadening, affecting both, vibronic and H-aggregate related spectral features.

The low energy spectral range (2.35-2.65 eV) of the spectrum for all analysed molecular films fits well with the H-aggregate absorption in solution. However, the aggregate-related spectral feature in merocyanine films with $PC_{61}BM$ is substantially reduced compared to neat films. The aggregation reduction is caused by the intermixing between $PC_{61}BM$ and merocyanine molecules, which is more pronounced in the branched merocyanine **MB**:$PC_{61}BM$ (Fig. 1d), indicating a higher degree of intermixing with $PC_{61}BM$ compared with the linear merocyanine **ML**:$PC_{61}BM$ blend (Fig. 1 c).

Molecular intermixing could also substantially alter the charge transport properties in bulk heterojunction (BHJ) solar cells[39]. We found that devices made with **ML** have better performance than **MB**-based devices: higher power conversion efficiency (PCE; 4.09% versus 1.66%) and fill factor (FF; 0.68 versus 0.42). As expected V_{OC} was similar in both cases. Further, the hole mobility of the blends as determined in an OFETs geometry was found to be higher in the **ML**-based device ($1.5*10^{-5}$ cm^2/Vs) as compared to $1.4*10^{-7}$ cm^2/Vs in an **MB**-based device. This also correlated with a stronger H-aggregation, observed in the absorption spectrum (Fig 1c,d).

Additionally, in the **MB**:$PC_{61}BM$ film, the 0-0 vibronic transition is spectrally broadened to the red side as compared to the **ML**:$PC_{61}BM$ film, could be a weak underlying transition below the 0-0 peak or a broadening effect. Ussualy in BHJ films, a new low energy state can be caused by hybridization of the D:A excited states wave functions, leading to a CT state formation.[40] To shed more light on the photophysical processes involving this transition, time-resolved transient absorption (TA) experiments as well as first-principles calculations were performed.

For the TA experiments, a 3 eV pulse was used for the optical excitation. With this photon energy, excitons can be generated both in $PC_{61}BM$ and in merocyanine molecules (see Fig. 1). Using a visible light continuum as a probe, we were able to directly monitor the dynamics.

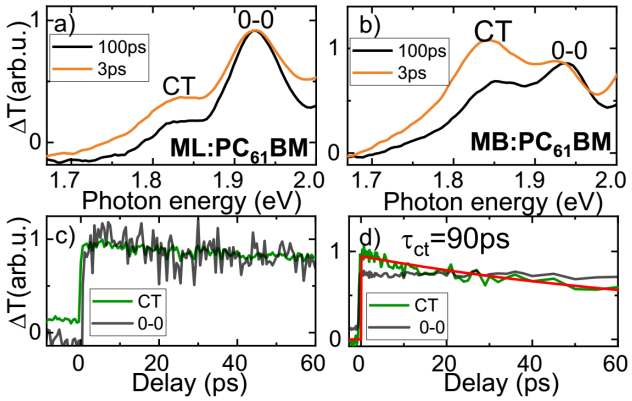

Figure 2: Time-resolved absorption spectra of a) **ML**:$PC_{61}BM$ and b) **MB**:$PC_{61}BM$ films at 3 ps (orange lines) and 100 ps (black lines) after excitation. The CT and the 0-0 ground state bleach (GSB) transitions are highlighted. Decay of the CT and 0-0 GSB signals of c) **ML**:$PC_{61}BM$ and d) **MB**:$PC_{61}BM$. A 90ps decaying exponential fit of the CT state is displayed in d) (red).

The results of time-resolved absorption spectroscopy are shown in Fig. 2. The spectral component at 1.92 eV is the ground state bleach (GSB) of the 0-0 vibronic replica and can be used to directly monitor the excitation dynamics on the merocyanine aggregates and molecules in a film.

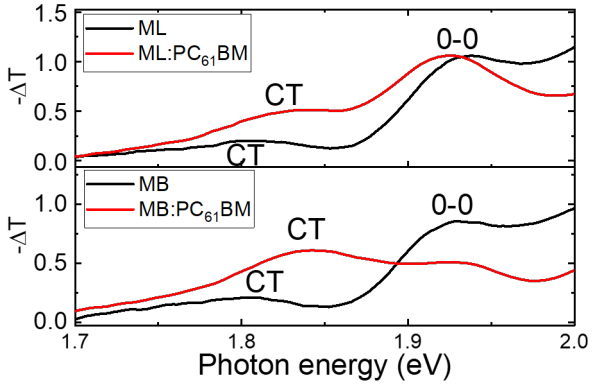

Figure 3 Transient absorption spectrum of pure and mixed films of A) ML and B) MB measured at 3 ps after the excitation using 3

eV excitation energy. All studied films have shown the CT state transition at 1.8-1.85 eV by means of stimulated emission process. 0-0 represents the ground state bleach signal of the 0-0 vibronic peak

An additional transient component at 1.85 eV was observed in both time resolved spectra. As further explained in the computational modelling section, the 1.85 eV transition was assigned to a state featuring an inter-molecular CT character amongst two merocyanine molecules. Similar CT excitons were previously suggested for a less dipolar merocyanine, however never modelled before.[41] The amplitude of this component in **ML**:$PC_{61}BM$ film is larger than the GSB component at 1.92 eV (Fig 2a). The transient signal below the absorption edge of the materials indicates a stimulated emission nature, which usually appears in the region where sample is luminescent. In the case of merocyanine dyes, luminescence at energies below the 0-0 transition is possible.

The amplitude of the CT state in TA spectrum is stronger in **MB**:$PC_{61}BM$ than in the ML:$PC_{61}BM$ film (Fig. 2a,b). This finding could indicate either a different oscillator strengths or different populations. Based on the absorption spectra (Fig. 1c,d) we assume that the oscillator strength is the dominant factor, because the 0-0 transition in the **MB**:$PC_{61}BM$ is slightly asymmetric compared to **ML**:$PC_{61}BM$. Different CT oscillator strengths in BHJ films could be caused by a different molecular packing also observed in terms of different H-aggregation properties.

Another aspect which distinguishes the two molecules from each other is the population dynamics of the CT state (Fig.2 c,d). The decay time of the CT state and the 0-0 bleach in **ML**:$PC_{61}BM$ films show no differences (130 ps), whereas in the **MB**:$PC_{61}BM$ they deviate at early times (20-30 ps after the excitation): while the CT state decays with 90 ps lifetime(Fig.1 d red), the 0-0 signal does not decay in the displayed 60ps time window (Fig.1). The high oscillator strength of the CT state suggests a strong wave-function overlap between electron and hole in the CT exciton. This would facilitate recombination between electrons and holes, giving rise to fast decay of the CT exciton. The 90 ps decay time could be associated to the relaxation to an intermediate state, for example a triplet state, because a direct recombination to the ground state would give a 90 ps recovery time in 0-0 transition, which was not observed experimentally.

Despite the limits of TDDFT in modelling correlation effects in the excited states, our simulations using a range-separated functional qualitatively agree with the experimental findings, providing a higher oscillator strength for the CT state in **MB**:$PC_{61}BM$ clusters than **ML**:$PC_{61}BM$ ones. This suggests that in blends with $PC_{61}BM$, the packing enhances the oscillator strength of the CT state for **MB** than **ML**.

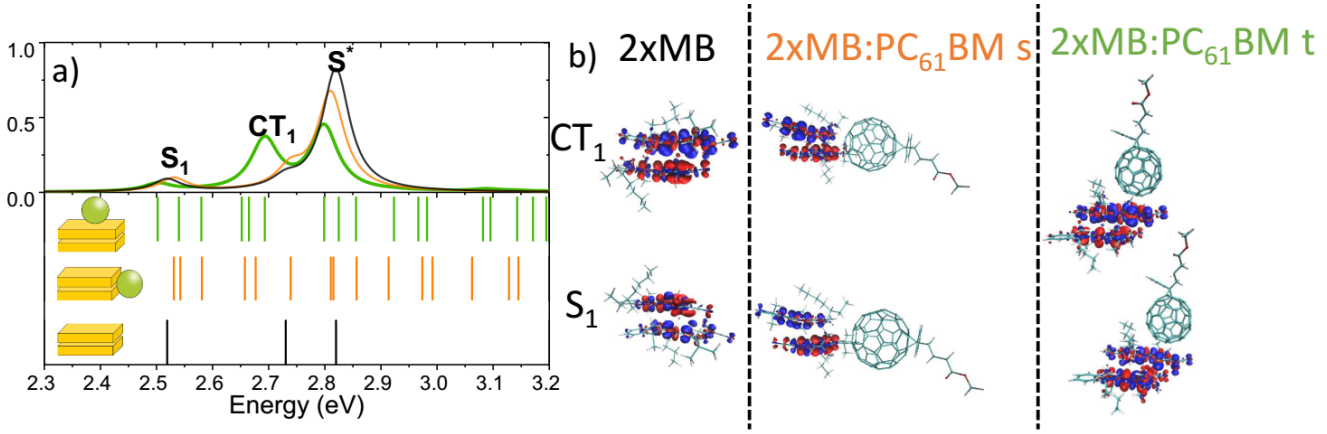

Figure 4: a): Computed TD-ωB97X-D3/6-31G* excited state vertical energies (unscaled values) for **MB** molecular clusters, namely: dimers (2x**MB**, black), dimer with $PC_{61}BM$ on top (2x**MB**:$PC_{61}BM$ t, green), dimer with $PC_{61}BM$ on side (2x**MB**:$PC_{61}BM$ s, orange). Absorption spectra plotted as convolution of Lorentzian functions. The label (*) represents the optically allowed excited state (in the text S*), here assigned to the 0-0 transition, as reported in Fig. 2. CT_1 or S_1 can either be assigned to the stimulated emission transition observed in the experiment at 1.85 eV (Fig. 2) b): electron-hole density plots for CT_1 and S_1 states for the three molecular clusters respectively.

In Fig. 4 are reported the TDDFT vertical transition energies (unscaled values) for the **MB** cases (see SI for values regarding **ML**), namely: the merocyanine dimer (2x**MB**) and the clusters with both on-top and on-side configurations (2x**MB**:$PC_{61}BM$ t, 2x**MB**:$PC_{61}BM$ s).

The merocyanine dimers are minimal structural models representing the pure merocyanine films, while the clusters with $PC_{61}BM$ the D:A interfaces. Both, **MB** and **ML** dimers, show a bright excited state, here referred to as S*, at similar energies and oscillator strengths (2.82 eV, f=1.54 for **MB** and 2.79 eV, f=1.95 for **ML**, respectively, see Fig. 4). S* can be assigned to the 0-0 absorption observed in the experiments (see Fig. 1). In the presence of $PC_{61}BM$, S* slightly shifts for both molecules, as a consequence of the inter-molecular interactions. Both, **MB** and **ML**, in dimers or in clusters with $PC_{61}BM$, show a

weak dipole-allowed low-energy state S_1. S_1 is more intense for **MB** than **ML** clusters. The analysis of the electron-hole densities (Fig. 4b) shows that S_1 can be described as a weak inter-molecular CT state between the two merocyanines. The presence of $PC_{61}BM$ does not significantly alter neither its character, nor the energy and oscillator strength.

Remarkably, an excited state showing a strong inter-molecular CT character between merocyanines, is predicted below S*. This state is named here CT_1 (see Fig. 4) and it is present for both on top ("face-on") and on side ("edge-on") $PC_{61}BM$ clusters. It derives from the CT_1 transition already present in the pure merocyanine dimer. CT_1 shows a clear electron-hole density separation, localized on the merocyanine domain. Furthermore, its energy, oscillator strength and partial charges are highly affected by the relative position of the $PC_{61}BM$. For the on-top $PC_{61}BM$ configuration in **MB** cluster, higher stabilization energy and oscillator strength for CT_1 are computed than the on-side (Fig. 4). For the case of **ML** clusters, the computed TDDFT energy for the CT state is higher than S* (see SI for details), and any clear CT state could be located below the optical allowed transition. This aspect might be due to various reasons: i) different local packing and dimer geometries, as induced by different alkyl side chains, ii) a small cluster size considered in the simulations, which is not sufficient for a full description of the electronic structure of **ML**:$PC_{61}BM$ cases. For such reasons, the computed data related to **ML** clusters are reported in SI, and further computational investigations will be needed to systematically address this point.

Comparing the TDDFT calculations with the experimental data (i.e., by shifting the computed energies), for the case of **MB** we can associate the CT_1 to the stimulated emission band observed at 1.85 eV (see Fig. 2). This state is predicted both, in pure **MB** and in **MB**:$PC_{61}BM$ clusters, as also experimentally observed. Because of the aforementioned TDDFT limits in computing the energies of the merocyanine excited states, we cannot completely exclude that the stimulated emission signals might also be assigned to the S_1 state, which shows a weak CT character as well (Fig. 4 b). We point out that our models are kept minimal, however, we do not exclude the appearance of further low-lying CT states, surrounding the optical gap (S*), the more we increase the cluster size. Similar effects have been reported in the literature for oligothiophene:$PC_{61}BM$ clusters[42].

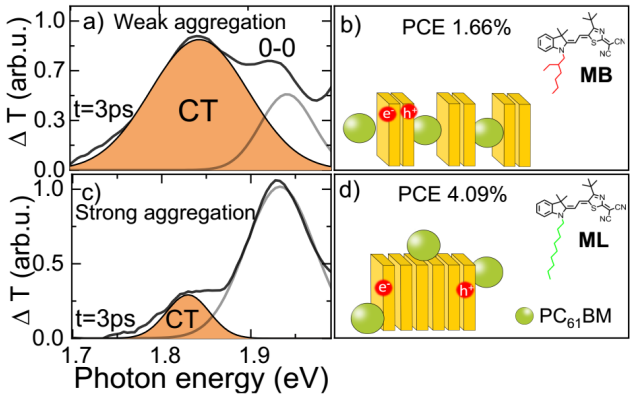

Figure 4: Transient absorption spectra at 3 ps delay of **MB** (a) and **ML** (c) blends with $PC_{61}BM$. Two Gaussian functions represent 0-0 and CT state transitions. Proposed packing model of **MB** (b) and **ML** clusters (d) in a blend with $PC_{61}BM$.

Both, modelling and experiments, suggest that the molecular geometry and packing can alter the photo-physics of merocyanine molecules blended with $PC_{61}BM$. An "on-top" configuration between $PC_{61}BM$ and merocyanine increases the oscillator strength of the CT state as compared to the "on-side" orientation. This can be caused by the different electron-hole delocalization and spatial wave-function overlap. In fact, for the "on-top" case the electron-hole overlap is slightly larger than the "on-side" cluster, thus leading to a less delocalised CT exciton, therefore to a higher oscillator strength for the CT transition (Fig. 4).

A sketch of molecular packing behaviour of **MB** and **ML** merocyanines is shown in Fig. 5. The amplitudes of the proposed CT state transitions (fitted using Gaussian distribution functions) are shown in the transient spectra of two different merocyanines at 3 ps delay. The strong H-aggregation and low intermixing between **ML** and $PC_{61}BM$ favours the "on edge" configuration, thus leading to a more delocalized CT state showing a weaker oscillator strength (Fig 4 c, d). The good intermixing of **MB**:$PC_{61}BM$ reduced the H-aggregation. This enables a more "on top" configuration, which decreases the CT delocalisation, therefore increasing the oscillator strength of the CT band (Fig 4 a, b). CT excitons in merocyanine clusters with a stronger H-aggregation are more delocalized and are easier to split into charge pairs, which leads a to better device performance.

Conclusions.

In this study experimental and first principles approaches were used to investigate the changes induced by the molecular packing on the intermolecular charge transfer state in terms of optical activity (i.e., oscillator strength) and decay dynamics. For this purpose, two merocyanines with identical core, but different alkyl side chains (i.e. branched *vs.* linear) were considered. Using absorption spectroscopy H-aggregation in liquid and solid phases was analysed and similar packing behaviour for both merocyanines was observed. By blending **ML** and **MB** merocyanines with $PC_{61}BM$, remarkable differences in the aggregation properties were observed, correlating with different D:A intermixing. Time resolved absorption studies showed the existence of an intermolecular CT state between merocyanine molecules showing strong molecular packing dependency. DFT and TDDFT calculations revealed how different merocyanines/$PCB_{61}M$ interfaces impact on the excited-state energies and dipole activities. Large enhancement of the CT state transition when $PC_{61}BM$ is positioned "on top" of the parallel aligned merocyanine cluster was found. This enhancement was explained as a change in the electron-hole overlap and delocalisation of the CT state. Our conclusion is evidenced by performance of solar cells and charge transport investigations.

AUTHOR INFORMATION

Corresponding Authors

pvl@ph2.uni-koeln.de; klaus.meerholz@uni-koeln.de

ACKNOWLEDGMENT

We acknowledge funding by the excellence initiative at the University of Cologne, key profile area “Quantum Matter and Materials (QM2)”.

REFERENCES

(1) Liu, Y.; Zhao, J.; Li, Z.; Mu, C.; Ma, W.; Hu, H.; Jiang, K.; Lin, H.; Ade, H.; Yan, H. Aggregation and Morphology Control Enables Multiple Cases of High-Efficiency Polymer Solar Cells. *Nat. Commun.* **2014**, *5* (1), 5293.

(2) Chen, X.-K.; Ravva, M. K.; Li, H.; Ryno, S. M.; Brédas, J.-L. Effect of Molecular Packing and Charge Delocalization on the Nonradiative Recombination of Charge-Transfer States in Organic Solar Cells. *Adv. Energy Mater.* **2016**, *6* (24), 1601325.

(3) Hutchison, G. R.; Ratner, M. A.; Marks, T. J. Intermolecular Charge Transfer between Heterocyclic Oligomers. Effects of Heteroatom and Molecular Packing on Hopping Transport in Organic Semiconductors. *J. Am. Chem. Soc.* **2005**, *127* (48), 16866–16881.

(4) Marchiori, C. F. N.; Koehler, M. Dipole Assisted Exciton Dissociation at Conjugated Polymer/Fullerene Photovoltaic Interfaces: A Molecular Study Using Density Functional Theory Calculations. *Synth. Met.* **2010**, *160* (7–8), 643–650.

(5) Verlaak, S.; Beljonne, D.; Cheyns, D.; Rolin, C.; Linares, M.; Castet, F.; Cornil, J.; Heremans, P. Electronic Structure and Geminate Pair Energetics at Organic-Organic Interfaces: The Case of Pentacene/C 60 Heterojunctions. *Adv. Funct. Mater.* **2009**, *19* (23), 3809–3814.

(6) Eisfeld, A.; Briggs, J. S. The J- and H-Bands of Organic Dye Aggregates. *Chem. Phys.* **2006**, *324* (2–3), 376–384.

(7) Balzer, F.; Rubahn, H. G. Growth Control and Optics of Organic Nanoaggregates. *Adv. Funct. Mater.* **2005**, *15* (1), 17–24.

(8) Liess, A.; Lv, A.; Arjona-Esteban, A.; Bialas, D.; Krause, A.-M. M.; Stepanenko, V.; Stolte, M.; Würthner, F. Exciton Coupling of Merocyanine Dyes from H- to J-Type in the Solid State by Crystal Engineering. *Nano Lett.* **2017**, *17* (3), 1719–1726.

(9) Xu, J.; Semin, S.; Niedzialek, D.; Kouwer, P. H. J.; Fron, E.; Coutino, E.; Savoini, M.; Li, Y.; Hofkens, J.; Uji-I, H.; et al. Self-Assembled Organic Microfibers for Nonlinear Optics. *Adv. Mater.* **2013**, *25* (14), 2084–2089.

(10) Dalton, L. R.; Sullivan, P. A.; Bale, D. H. Electric Field Poled Organic Electro-Optic Materials: State of the Art and Future Prospects. *Chem. Rev.* **2010**, *110* (1), 25–55.

(11) Jiang, Y.; Gindre, D.; Allain, M.; Liu, P.; Cabanetos, C.; Roncali, J. A Mechanofluorochromic Push-Pull Small Molecule with Aggregation-Controlled Linear and Nonlinear Optical Properties. *Adv. Mater.* **2015**, *27* (29), 4285–4289.

(12) Bakulin, a. a.; Dimitrov, S. D.; Rao, a.; Chow, P. C. Y.; Nielsen, C. B.; Schroeder, B. C.; McCulloch, I.; Bakker, H. J.; Durrant, J. R.; Friend, R. H. Charge-Transfer State Dynamics Following Hole and Electron Transfer in Organic Photovoltaic Devices. *J. Phys. Chem. Lett.* **2013**, *4* (1), 209–215.

(13) Ran, N. A.; Roland, S.; Love, J. A.; Savikhin, V.; Takacs, C. J.; Fu, Y.-T.; Li, H.; Coropceanu, V.; Liu, X.; Brédas, J.-L.; et al. Impact of Interfacial Molecular Orientation on Radiative Recombination and Charge Generation Efficiency. *Nat. Commun.* **2017**, *8* (1), 79.

(14) Adil, M. A.; Zhang, J.; Deng, D.; Wang, Z.; Yang, Y.; Wu, Q.; Wei, Z. Modulation of the Molecular Orientation at the Bulk Heterojunction Interface via Tuning the Small Molecular Donor-Nonfullerene Acceptor Interactions. *ACS Appl. Mater. Interfaces* **2018**, *10* (37), 31526–31534.

(15) Ojala, A.; Petersen, A.; Fuchs, A.; Lovrincic, R.; Pölking, C.; Trollmann, J.; Hwang, J.; Lennartz, C.; Reichelt, H.; Höffken, H. W.; et al. Merocyanine/C60 Planar Heterojunction Solar Cells: Effect of Dye Orientation on Exciton Dissociation and Solar Cell Performance. *Adv. Funct. Mater.* **2012**, *22* (1), 86–96.

(16) Zhang, L.; Roy, S. S.; Hamers, R. J.; Arnold, M. S.; Andrew, T. L. Molecular Orientation-Dependent Interfacial Energetics and Built-in Voltage Tuned by a Template Graphene Monolayer. *J. Phys. Chem. C* **2015**, *119* (1), 45–54.

(17) Tumbleston, J. R.; Collins, B. A.; Yang, L.; Stuart, A. C.; Gann, E.; Ma, W.; You, W.; Ade, H. The Influence of Molecular Orientation on Organic Bulk Heterojunction Solar Cells. *Nat. Photonics* **2014**, *8* (5), 385–391.

(18) Chen, W.; Qi, D. C.; Huang, H.; Gao, X.; Wee, A. T. S. Organic-Organic Heterojunction Interfaces: Effect of Molecular Orientation. *Adv. Funct. Mater.* **2011**, *21* (3), 410–424.

(19) Würthner, F.; Yao, S. Dipolar Dye Aggregates: A Problem for Nonlinear Optics, but a Chance for Supramolecular Chemistry. *Angew. Chemie Int. Ed.* **2000**, *39* (11), 1978–1981.

(20) Würthner, F.; Yao, S.; Debaerdemaeker, T.; Wortmann, R. Dimerization of Merocyanine Dyes. Structural and Energetic Characterization of Dipolar Dye Aggregates and Implications for Nonlinear Optical Materials. *J. Am. Chem. Soc.* **2002**, *124* (32), 9431–9447.

(21) Rösch, U.; Yao, S.; Wortmann, R.; Würthner, F. Fluorescent H-Aggregates of Merocyanine Dyes. *Angew. Chemie Int. Ed.* **2006**, *45* (42), 7026–7030.

(22) Yao, S.; Beginn, U.; Gress, T.; Lysetska, M.; Würthner, F. Supramolecular Polymerization and Gel Formation of Bis(Merocyanine) Dyes Driven by Dipolar Aggregation. *J. Am. Chem. Soc.* **2004**, *126* (26), 8336–8348.

(23) Lohr, A.; Grüne, M.; Würthner, F. Self-Assembly of Bis(Merocyanine) Tweezers into Discrete Bimolecular π-Stacks. *Chem. - A Eur. J.* **2009**, *15* (15), 3691–3705.

(24) Le Guennic, B.; Jacquemin, D. Taking Up the Cyanine Challenge with Quantum Tools. *Acc. Chem. Res.* **2015**, *48* (3), 530–537.

(25) Ghosh, S.; Verma, P.; Cramer, C. J.; Gagliardi, L.; Truhlar, D. G. Combining Wave Function Methods with Density Functional Theory for Excited States. *Chem. Rev.* **2018**, *118* (15), 7249–7292.

(26) Brückner, C.; Engels, B. Benchmarking Singlet and Triplet Excitation Energies of Molecular Semiconductors for Singlet Fission: Tuning the Amount of HF Exchange and Adjusting Local Correlation to Obtain Accurate Functionals for Singlet–Triplet Gaps. *Chem. Phys.* **2017**, *482*, 319–338.

(27) Capobianco, A.; Borrelli, R.; Landi, A.; Velardo, A.; Peluso, A. Absorption Band Shapes of a Push–Pull Dye Approaching the Cyanine Limit: A Challenging Case for First Principle Calculations. *J. Phys. Chem. A* **2016**, *120* (28), 5581–5589.

(28) Frisch, M. J.; Trucks, G. W.; Schlegel, H. B.; Scuseria, G. E.; Robb, M. A.; Cheeseman, J. R.; Scalmani, G.; Barone, V.; Petersson, G. A.; Nakatsuji, H.; et al. Gaussian 16 Revision B.01. 2016.

(29) Giannozzi, P.; Baroni, S.; Bonini, N.; Calandra, M.; Car, R.; Cavazzoni, C.; Ceresoli, D.; Chiarotti, G. L.; Cococcioni, M.; Dabo, I.; et al. QUANTUM ESPRESSO: A Modular and Open-Source Software Project for Quantum Simulations of Materials. *J. Phys. Condens. Matter* **2009**, *21* (39).

(30) Ge, X.; Binnie, S. J.; Rocca, D.; Gebauer, R.; Baroni, S. TurboTDDFT 2.0—Hybrid Functionals and New Algorithms within Time-Dependent Density-Functional Perturbation Theory. *Comput. Phys. Commun.* **2014**, *185* (7), 2080–2089.

(31) Guerrini, M.; Calzolari, A.; Corni, S. Solid-State Effects on the Optical Excitation of Push–Pull Molecular J-Aggregates by First-Principles Simulations. *ACS Omega* **2018**, *3* (9), 10481–10486.

(32) Gsänger, M.; Bialas, D.; Huang, L.; Stolte, M.; Würthner, F. Organic Semiconductors Based on Dyes and Color Pigments. *Adv. Mater.* **2016**, *28* (19), 3615–3645.

(33) Mustroph, H.; Reiner, K.; Mistol, J.; Ernst, S.; Keil, D.; Hennig, L. Relationship between the Molecular Structure of Cyanine Dyes and the Vibrational Fine Structure of Their Electronic Absorption Spectra. *ChemPhysChem* **2009**, *10* (5), 835–840.

(34) Maryott, A. A.; Smith, E. R. *Table of Dielectric Constants of Pure Liquids*; 1951.

(35) Kasha, M.; Rawls, H. R.; Ashraf El-Bayoumi, M. The Exciton Model in Molecular Spectroscopy. *Pure Appl. Chem.* **1965**, *11* (3–4), 371–392.

(36) Davydov, A. S. The Theory of Molecular Excitons. *Sov. Phys. Uspekhi* **1962**, *7* (2), 145–178.

(37) Nüesch, F.; Grätzel, M. H-Aggregation and Correlated Absorption and Emission of a Merocyanine Dye in Solution, at the Surface and in the Solid State. A Link between Crystal Structure and Photophysical Properties. *Chem. Phys.* **1995**, *193* (1–2), 1–17.

(38) Ryu, N.; Okazaki, Y.; Pouget, E.; Takafuji, M.; Nagaoka, S.; Ihara, H.; Oda, R. Fluorescence Emission Originated from the H-Aggregated Cyanine Dye with Chiral Gemini Surfactant Assemblies Having a Narrow Absorption Band and a Remarkably Large Stokes Shift. *Chem. Commun.* **2017**, *53* (63), 8870–8873.

(39) Würthner, F.; Meerholz, K. Systems Chemistry Approach in Organic Photovoltaics. *Chem. - A Eur. J.* **2010**, *16* (31), 9366–9373.

(40) Ragoussi, M.-E.; Torres, T. Organic Photovoltaics. *Rev. Virtual Química* **2015**, *7* (1), 112–125.

(41) Peckus, D.; Devižis, A.; Augulis, R.; Graf, S.; Hertel, D.; Meerholz, K.; Gulbinas, V. Charge Transfer States in Merocyanine Neat Films and Its Blends with [6,6]-Phenyl-C 61 -Butyric Acid Methyl Ester. *J. Phys. Chem. C* **2013**, *117* (12), 6039–6048.

(42) Fazzi, D.; Barbatti, M.; Thiel, W. Hot and Cold Charge-Transfer Mechanisms in Organic Photovoltaics: Insights into the Excited States of Donor/Acceptor Interfaces. *J. Phys. Chem. Lett.* **2017**, *8* (19), 4727–4734.

For table of Contents Only